NRIAG Journal of Astronomy and Geophysics 6 (2017) 174–183

Contents lists available at ScienceDirect

NRIAG Journal of Astronomy and Geophysics

journal homepage: www.elsevier.com/locate/nrjag

Full length article

Geophysical exploration to estimate the surface conductivity of residual argillaceous bands in the groundwater repositories of coastal sediments of EOLGA, Nigeria

N.J. George [a,*], J.G. Atat [b], E.B. Umoren [b], Isong Etebong [a]

[a] Akwa Ibom State University, Ikot Akpaden, Nigeria
[b] University of Uyo, Uyo, Nigeria

ARTICLE INFO

Article history:
Received 12 October 2016
Revised 24 January 2017
Accepted 7 February 2017
Available online 1 March 2017

Keywords:
Archie's law
Coastal aquifer
Electrical conductivity
Residual argillaceous bands

ABSTRACT

Electrical geophysical applications exploit a petrophysical relationship governing the electrical properties of rocks/sediments when field data are coupled with laboratory data. Given the robust analytical techniques of electrical method and the interrelationship with laboratory measurements, it seems natural to classify, and hence simplify, the spatially aggregated conductivity information on the basis of rock/sediment lithology. This provides a unique link between lithological sediment/rock parameters and the physical parameters controlling bulk conductivity. In this work vertical electrical sounding (VES) technique employing Schlumberger configuration integrated with sediment and water analysis have been used to determine the conductivity of argillaceous bands of aquifer sands (fine- coarse sands) in Eastern Obolo Local Government Area (EOLGA). The analysis of the data shows that the aquifer systems composing of fine sands, siltstones and coarse sand have bulk and pore-water resistivities ranging from 40.1–2049.4 Ω m (average = 995.18 Ω m) to 2.7–256.9 Ω m (average = 91.2 Ω m) respectively. These ranges respectively correspond to porosity and formation factor of (19.5–40.6%; average = 29.2%) and (7.1–19.7%; average = 12.95%). Within the limit of experimental errors clearly specified in the work, the intrinsic (clay-free) formation factor (F_i) was estimated to be 16.34 while the intrinsic porosity and the conductivity of the pore-scale clay (σ_A) were respectively estimated to be 20.4% and 3.2679 mS/m. Accounting for this conductivity magnitude of argillaceous bands from bulk conductivity (σ_b) of aquifer sands makes the aquifer systems in the area to be consistent with Archie's law that is valid only in clay-free sandy formation. The graphical deductions and contour distribution of parameters realised from data processing could be used to derive input parameters for contaminant migration modelling and to improve the quality of model in the study area.

1. Introduction

The sediments of the aquifer repository of Eastern Obolo Local Government Area (EOLGA) and the surrounding zones are often assumed to be shale-clay free (i.e. Archie's model compliant) since the greater percentage of the Coastal Plain sands (Benin Formation) is fine-coarse sands. This assumption to some extent reduces the validity of the results of any parameters searched for, because of the significant effect of argillites in the formations. In practice, even the cleanest formations often contain small amounts of clay, or argillaceous bands, which can exert a significant influence on bulk conductivity. The presence of clay minerals in many rocks puts additional charge carriers in the fluid adjacent to solid surfaces, causing additional conduction along the surface, which is confined to a thin layer known as the electric double layer (Soupios et al., 2007; George et al., 2015).

Resistivity methods are widely used as an aid to locate water-supply boreholes in basement and sedimentary terrains. Adverse conditions or anomalies due to geologic variation of layers can be

* Corresponding author.
E-mail addresses: Nyaknojimmyg@gmail.com, nyaknojimmyg@yahoo.com, nyaknogeorge@aksu.edu.ng (N.J. George).

Peer review under responsibility of National Research Institute of Astronomy and Geophysics.

Production and hosting by Elsevier

http://dx.doi.org/10.1016/j.nrjag.2017.02.001
2090-9977/

identified readily while specific targets such as thin conductive zones may be missed. Quantitative interpretation may be less reliable than is often assumed. The combination of geophysical data and laboratory analysis of the real geologic materials under observation can comfortably help in realising the targets being sought for. Assumption of the local geological setting may not always be appropriate and resources should be targeted on districts where problems can be solved. Qualitative interpretations are adequate in some situations but more rigorous field procedures and analytical techniques are needed to ensure that useful hydrogeological information is obtained (Carothers, 1986; Ibanga and George, 2016)

In sediments, which conduct electronically, formation conductivity is related to the volume and conductivity of the water in earth materials. The groundwater conducts through its ions, and its conductivity, therefore, depends strongly on the total dissolved solids. Within a porous, clay-free medium whose matrix is non-conducting, a relationship in Eq. (1), known as Archie's Law (Archie, 1942) is widely used and reasonably valid:

$$\frac{\sigma_w}{\sigma_f} = F = \frac{a}{\phi^m} \tag{1}$$

where σ_w, σ_f, F, a, m and ϕ are conductivity of water, conductivity of formation as a whole, formation factor (related to volume and tortuosity), pore geometry factor (typically 1 for unconsolidated sediments), Archie's cementation factor (typically 2 for unconsolidated sediments) and formation effective porosity respectively. Although the groundwater repository (usually sandy) is theoretically assumed to be clay-free, in practice, there is a considerably amount of argillaceous bands as evidenced in the noticed traces of clay/silt in some borehole lithologies.

The purpose of the present study is to review and understand the petrophysical information contained in integrating electrical resistivity method and laboratory analysis of sediments. The pore fluid obtained from the geologic sediment enabled in gauging the surface electrical resistivity/conductivity of the usually ignorable thin argillite within the aquifer sediments of EOLGA. Even though borehole screens are not seated in clay formation during borehole development, the flow of clay within and in between the aquifer repositories can induce extraneous conductivity into open aquifer that characterises the aquifer systems of the area. The induced conductivity will then influence many parameters such as effective porosity, formation factor, resistivity and tortuosity (τ), which relates to porosity and formation factor as in Eq. (2):

$$\tau = (F\phi)^{\frac{1}{2}} \tag{2}$$

Since these factors are useful in contaminant flow study and in groundwater modelling, the need to assess the level of the latent residual surface conductance in groundwater repositories is paramount.

2. Determination of porosity from intrinsic formation factor

An empirically based relationship exists in many rocks between the formation bulk electrical resistivity ρ_b, fractional porosity ϕ and specific resistivity of the saturating fluid ρ_w. This relationship which is a modified form of Eq. (1) was first used by Archie (1942) and is now a fundamental law that can be stated as

$$\rho_b = a \cdot \rho_w \cdot \phi^{-m} \tag{3}$$

where a is a formation dependent parameter whose value is usually assumed to be unity (valid if the rock matrix is perfectly insulating) although in many geologic formations, its actual value is known to depart from the assumed unity value. Technically, the constant a signifies the ease with which the mineral grains permit the free flow of electric current through it (Soupios et al., 2007; Aristodemou and Thomas-Betts, 2000; Slater, 2007; Kirsch, 2009). The material constant m has several interpretations including porosity exponent, shape cementation factor, grain-shape and pore-shape factor (Khalil and Abd-Alla, 2005) The values of m depend on many factors including pore shape geometry, extent of compaction, mineral composition and the insolating properties of the cementation (Khalil and Abd-Alla, 2005; Ransom, 1984; George et al., 2015). Other factors include overburden pressure and anisotropy. Typical range of values of a and m for different geologic formations have been published by many researchers including (Hill and Milburn, 1956; Schön, 1996) and wide variations have been observed.

In an idealised saturated clean sand environment where the mineral grains are assumed to be perfectly insulating, the concept of intrinsic formation factor, F_i which is technically defined as $\frac{\rho_o}{\rho_w}$ (ρ_o is the resistivity of the saturated rock) has been introduced. The intrinsic porosity ϕ_i is related to F_i and other formation parameters as

$$\phi_i = e^{\frac{1}{m}\ln(a)+\frac{1}{m}\ln\left(\frac{1}{F_i}\right)} \tag{4}$$

Since the values of a and m vary according to changes in pore geometry, it therefore becomes necessary that their values are determined at each site so as to be in conformity with the prevailing subsurface conditions at the site. Consequently, Archie is not a universal law, it is just an empirical equation for certain cases because several factors can influence the resistivity predicted from Archie's law. Such factors include the presence of sources of internal surface conductivity like the clay content of the formation and the existence of clay minerals within the pore spaces (Keller and Frischknecht, 1966). Also if subsurface structures like faults and fractures exist in the formation, their presence can either decrease the bulk resistivity predicted from Archie's law if such structures are opened and filled with some conductive fluids like water or increase the bulk resistivity of the formation if those fractures and faults are opened and filled with insulating materials like air that will not permit free flow of electrical current through them (Benkabbour et al., 2004). Also formation resistivities predicted from Archie's law will not be realised in locations where poorly conducting fluids like some forms of chlorinated dense nonaqueous phase liquids (DNAPLs) (for instance trichloroethene) contaminate the saturated aquifer environment (Tait et al., 2004; Rivett and Clark, 2007; Chambers et al., 2010) partially saturated aquifer (Alger, 1966) and fresh water aquifer (Huntley, 1987). In such geologic environments and subsurface conditions, an additional corrective term that will account for the additional sources of conductivity is required. A large number of such models are currently in use and majority of them fall into either shale-fraction or cation-exchange model derived empirically using the concept of parallel conduction (Waxman and Smits, 1968; Sen et al., 1998; Frohlich and Urish, 2002; George et al., 2015).

The Waxman-Smits model which is a modified version of Archie's law is a common choice when describing the flow of current in aquifer systems where the original version of Archie's law has been violated by additional sources of subsurface conductivity (Soupios et al., 2007; Vinegar and Waxman, 1984). Soupios et al. (2007) and Worthington (1993) reported that in the Waxman-Smits's model, the apparent and intrinsic formation factors, (F_a (the ratio of bulk resistivity to fluid resistivity) and F_i (the same ratio after taking into account the shale effects)) are related according to Eq. (5) as

$$F_a = \frac{F_i}{1 + BQ_v\rho_w} \tag{5}$$

where B and Q_v indicate the equivalent conductance of the sodium clay-exchange cation as a function of formation water conductivity and cation exchange capacity of the rock per unit volume respectively. These parameters convey valuable information on the influence of subsurface condition on electric current flow. Eq. (5) can be transformed into a linear form as

$$\frac{1}{F_a} = \frac{1}{F_i} + \left(\frac{BQ_v}{F_i}\right)\rho_w \tag{6}$$

From Eq. (6), F_i can be obtained from the inverse of the intercept along the $\frac{1}{F_a}$ axis when a graph of $\frac{1}{F_a}$ against ρ_w is plotted while BQ_v can be determined from the slope-intercept relationship of the same graph. Thus by graphically plotting $\frac{1}{F_a}$ against ρ_w, F_i can be obtained and subsequently can be used in estimating the porosity of a clay-free medium in Eq. (4). This approach requires determining variations of ρ_o with depth in the formation from I-D inversion of resistivity data and ρ_w from water wells nearest to the VES stations (Soupios et al., 2007; Slater, 2007; Aristodemou and Thomas-Betts, 2000). From these two sets of data, the F_a of a water saturated aquifer can be computed. It is worth noting that in environments where the $BQ_v\rho_w$ term vanishes, F_a and F_i will be equal. That is

$$BQ_v\rho_w = 0 \tag{7}$$

Since ρ_w must be greater than 0, then it implies that it is the BQ_v term that will actually vanish. Thus from Eq. (6), it is obvious that a major source of error lies in wrong estimation of F_a.

It is important also to note that the factors which govern current flow and conductivity distribution in the soil (lithology, shape, mineralogy, packing and orientation of the mineral grains, shape and geometry of pores and pore channels, magnitude of porosity, tortuosity and permeability, compaction, consolidation and cementation and depth and water distribution) are highly variable (George et al., 2011a,b; Gomaa, 2013; Gomaa and Abou, 2015). Consequently, it should be expected that the measured and calculated formation parameters are not absolute but relative and therefore only relative conclusion about the area's formation parameters can be made (Vinegar and Waxman, 1984).

3. Location and geology of the study area

The study area pictorially represented in Fig. 1 lies between longitudes 7°30′E and 7°42′E and latitudes 4°15′N and 4°32′N in the Niger Delta region of southern Nigeria. The study area is located in an equatorial climatic region that is characterised by two major seasons. The seasons are the rainy season (March – October) and dry season (November – February) (Aristodemou and Thomas-Betts, 2000; George et al., 2010). The dry season is a period of extreme aridity characterized by excruciating high temperatures that do reach 35 °C. The area has been severely affected by the current global climatic changes in such a way that there have been shifts in both the upper and lower boundaries of these climatic conditions (Martínez et al., 2008; Rapti-Caputo, 2010; Riddell et al., 2010; Wagner and Zeckhauser, 2011; Farauta et al., 2012; George et al., 2015).

The study area is located in the Tertiary to Quaternary Coastal Plain Sands (CPS) (otherwise called the Benin Formation) and Alluvium environments of the Niger Delta region of southern Nigeria (Fig. 1). The Benin Formation which is underlain by the Parallic Agbada Formation covers over 80% of the study area. The sediments of the Benin Formation consist of interfringing units of lacustrine and fluvial loose sands, pebbles, clays and lignite streaks of varying thicknesses while the alluvial units comprise tidal and lagoonal sediments, beach sands and soils (Reijers and Petters, 1987; Nganje et al., 2007; George et al., 2014a,b) which are mostly found in the southern parts and along the river banks. The CPS is covered by thin lateritic overburden materials with varying thicknesses at some locations but is massively exposed near the shorelines. The CPS forms the major aquiferous units in the area. It comprises poorly sorted continental (fine-medium-coarse) sands and gravels that alternate with lignite streaks, thin clay horizons and lenses at some locations. The thin clay/shale horizons truncate the vertical and lateral extents of the sandy aquifers thereby building up multi-aquifer systems in the area (Edet and Worden, 2009; George et al., 2016b). Thus both confined and partially confined aquifers can be found in the area.

4. Material and method of analysis

4.1. Electrical resistivity method

Resistivity methods are widely used as an aid to locating water-supply boreholes in basement and sedimentary terrains. Adverse conditions or anomalies due to geologic variation of layers can be identified readily but specific targets such as narrow conductive zones may be missed mostly when the bedding plain is thin. Surface electrical methods have been used in investigating different types of geological, geotechnical and environmental problems for many years due to the dependence of earth resistivity on some geologic parameters. Details of this can be found in (Keller and Frischknecht, 1966; Zhdanov and Keller, 1994). Many electrode configurations and field procedures exist that can be used to perform geoelectrical investigations (Zhdanov and Keller, 1994) but the Schlumberger array which was performed using the vertical electrical sounding field procedure was adopted using the expression in Eq. (8) to assess the subsurface electrical resistivity and the depth of the economically accessible aquifers.

$$\rho_a = \pi \cdot \frac{\left(\frac{AB}{2}\right)^2 - \left(\frac{MN}{2}\right)^2}{(MN)} \cdot R_a \tag{8}$$

where ρ_a, AB, MN and R_a are apparent resistivity, current electrode spacing, potential electrode spacing and apparent resistance measured from Terrameter. The factor (G) given in the next equation which was multiplied by apparent resistance R_a, is called geometric factor and it depends on electrode configuration used.

$$G = \pi \cdot \frac{\left(\frac{AB}{2}\right)^2 - \left(\frac{MN}{2}\right)^2}{(MN)} \tag{9}$$

The electrical resistivity investigations were conducted in twelve (12) locations across the study area between 2012 and 2013 using a SAS1000 model of ABEM Terrameter. Maximum current electrode spacing (AB) was constrained by settlement pattern and other space limiting conditions to vary from one location to another. This confined the VES points to the locations shown in Fig. 1. In locations with good access paths and/or roads, the current cables were extended up to 1000 m in order to ensure that depths above 200 m were comfortably sampled assuming that penetration depth varies between $0.25AB$ and $0.5AB$ (Singh, 2005; Roy and Elliot, 1981; George et al., 2015).

Corresponding receiving or potential electrode separation (MN) varied from a minimum of 0.5 m at AB = 2 m to a maximum of 50 m at AB = 1000 m. At all the electrode positions, great care was taken to ensure that the separation between the potential electrodes did not exceed one fifth of the separation of the current electrodes (Gowd, 2004; George et al., 2015). VES data quality was generally good especially in the wet season but in the dry season, the electrode positions were usually wetted with water and salt solution (where necessary) in order to lower the contact resistance and

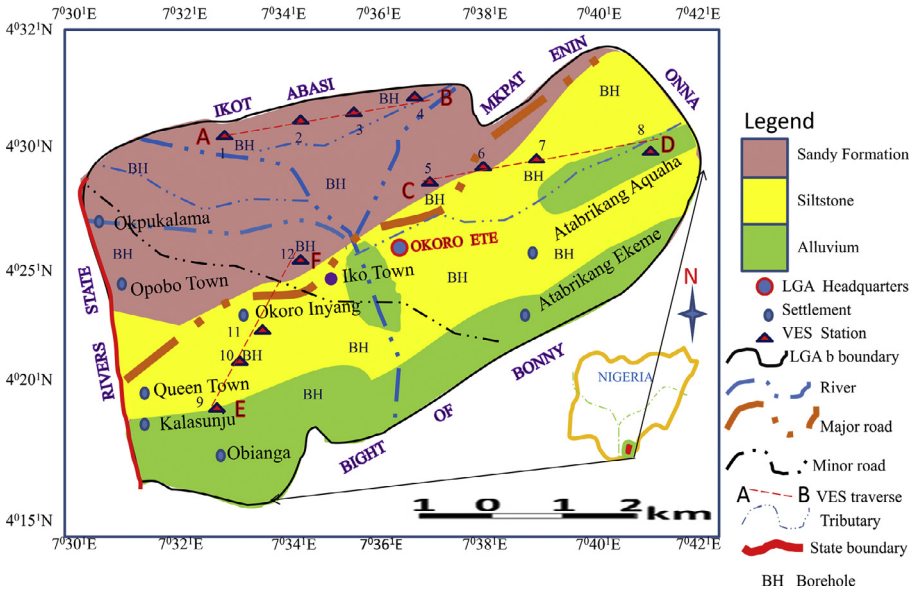

Fig. 1. Map showing generalised geology, VES transects and VES points of EOLGA of Akwa Ibom State, Nigeria (George et al., 2014a).

consequently ensure good electrical contact between the ground and the steel electrodes.

Information generated from the analyses of geophysical data was used to constrain drilling. The drilling phase started as soon as the geophysical reports were submitted to the Akwa Ibom State Millennium Development Goal (Akwa Ibom State Millennium Development Goal (AKSMDG, 2011)) that funded the borehole projects. Manual drilling technique was adopted in drilling 6 in. borehole in all locations since the subsurface condition in the entire area was favourable for such drilling method. Some of the boreholes were cited adjacent to the VES stations while some that are located at where there was no access path to spread the cables at the vicinity of the boreholes were separated by more than 150 m. The drill cuttings were logged geologically in all 12 locations and samples were collected for laboratory analysis. The drilled boreholes were cased using 75 mm high pressure PVC casing materials. The PVC casings were slotted at various depths and the slotted region of the well annulus was gravel packed to ensure good delivery of water to the borehole. Gravel packing is also important in checking the ingress of sediments into the borehole. A mixture of sand and cement was used to grout the boreholes to prevent back flow of water at the surface into the well (Gowd, 2004). The pumping test was performed by a 24 h pumping period and a 24 h recovery data collection (Gowd, 2004). Details of the procedures and analytical techniques adopted in the analyses of the pumping tests data can be found in Gowd (2004). Water samples were collected and *in situ* measurement of electrical conductivity was performed in all the boreholes using WTW LF91 conductivity metre.

4.2. Laboratory analysis of borehole sediments for determination of fractional porosity

The cored aquifer sediments were pre-washed with distilled water to remove traces of clay and other argillaceous materials that might have originated from the coring operation American Petroleum Institute (API, 1960). The samples were later put into a vacuum desiccator and evacuated at a pressure of 0.3 mBar for a period of 1 h (see Emerson, 1969). De-aerated distilled water was gently poured into the desicator until the water completely covers all the samples. All the samples were later soaked for a period of 24 h in order to ensure that any trace of salt and other related soluble contaminants within the samples diffused out into the surrounding water. The cleaned samples were later dried in a temperature controlled oven at 105 °C for 16 h in order to check any irreversible change in the composition of the samples (see Emerson, 1969; Galehouse, 1971). The oven dried core samples were allowed to cool to normal air temperature in a desicator. The weight of the cool and dry core samples W_d were measured using an electronic weighing balance five times and the mean computed and recorded. The samples were soaked with distilled water that has been boiled for 30 min in a vacuum pressure of 0.3 mBar for 18 h. The weight of the wet samples W_w was also measured five times and the mean computed and recorded. Effective porosity (ϕ) of the samples was calculated using Eq. (10) as

$$\phi = 100 \cdot \left(\frac{W_w - W_d}{V}\right)\% \tag{10}$$

where V is volume of the samples. Details of the experimental procedure can be found in API (API, 1960; Emerson, 1969).

4.3. Estimation of hydraulic conductivity

Using The Kozeny-Carman-Bear's Model (KCBM) equation which establishes a quantitative relationship between k with ϕ and other site dependent equations, the hydraulic conductivities for the different VES locations were estimated. The expression for KCBM equation is given in Eq. (11) as

$$k = \left(\frac{\delta_w g}{\mu_d}\right) \cdot \left(\frac{d_m^2}{180}\right) \cdot \left[\frac{\phi^3}{(1-\phi)^2}\right] \tag{11}$$

where δ_w is the density of water (taken as 1000 kg/m^3), d_m is the mean grain size of sediments which was determined in this study by direct measurement using Vernier Callipers and micrometer screw gauge to be 0.000348 m and μ_d is the dynamic viscosity of water which according to Fetters (1994) can be taken to be 0.0014 kg/ms. The computed aquifer porosity ϕ, aquifer bulk formation factor F_a, aquifer estimated hydraulic conductivities k, aquifer pore water resistivities, k. σ values for aquifer formation, VES location coordinates measured with Global positioning system (GPS) in the study (see Fig. 1) and aquifer VES primary parameters are shown in Table 1.

Table 1
Summary of aquifer petrophysical parameters.

VES NO	Bulk resistivity ρ_b (Ω m)	Pore-water resistivity ρ_w (Ω m)	Bulk formation factor, F_a	Depth to prolific aquifer (m)	$1/F_a$	Porosity ϕ (%)	Predicted hydraulic conductivity K (m/s)	Predicted hydraulic conductivity K (m/day)	$K \cdot \sigma$ (Ω^{-1} day^{-1})
1	549.2	47.8	11.5	52.7	0.08695	30.5	0.000158	13.65	0.02485
2	1913.0	214.9	9.0	114.0	0.11111	35.0	0.000238	20.56	0.01074
3	2049.4	149.6	13.7	67.4	0.07299	27.8	0.000119	10.28	0.00501
4	1464.5	124.1	11.5	20.6	0.08695	30.1	0.000152	13.13	0.00896
5	1362.2	100.9	13.5	82.9	0.07407	28.0	0.000122	10.54	0.00773
6	860.5	55.2	15.6	112.4	0.06410	26.0	0.00010	8.64	0.01004
7	52.6	2.7	19.7	82.9	0.05076	19.5	0.00004	3.46	0.06577
8	40.1	3.6	11.1	73.4	0.09009	31.2	0.000169	14.60	0.36409
9	393.9	28.3	13.9	91.8	0.07194	27.6	0.000117	10.10	0.02564
10	611.2	38.2	16.0	68.7	0.0625	25.6	0.00009	7.78	0.01272
11	924.2	72.2	12.8	110.9	0.07812	28.9	0.000134	11.58	0.01253
12	1721.4	256.9	7.1	115.1	0.14084	40.6	0.000372	32.140	0.01867

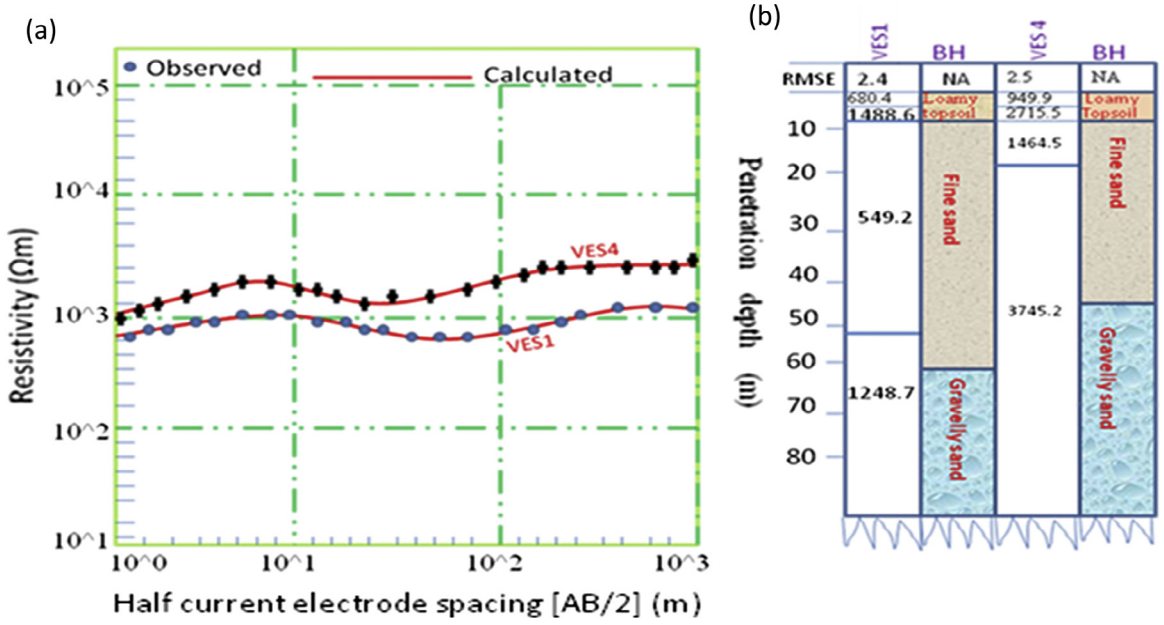

Fig. 2. Samples of modelled VES curves along AA profile (a) correlating between VES derived 1-D subsurface models and borehole lithologs (b).

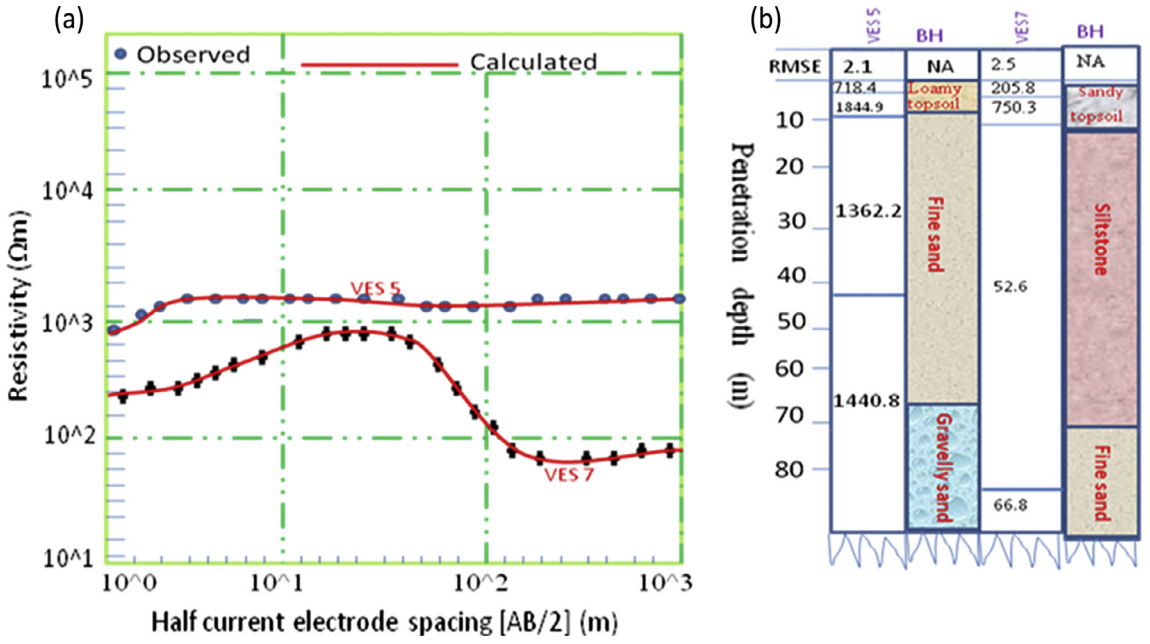

Fig. 3. Samples of modelled VES curves along BB profile (a) correlating between VES derived 1-D subsurface models and borehole lithologs (b).

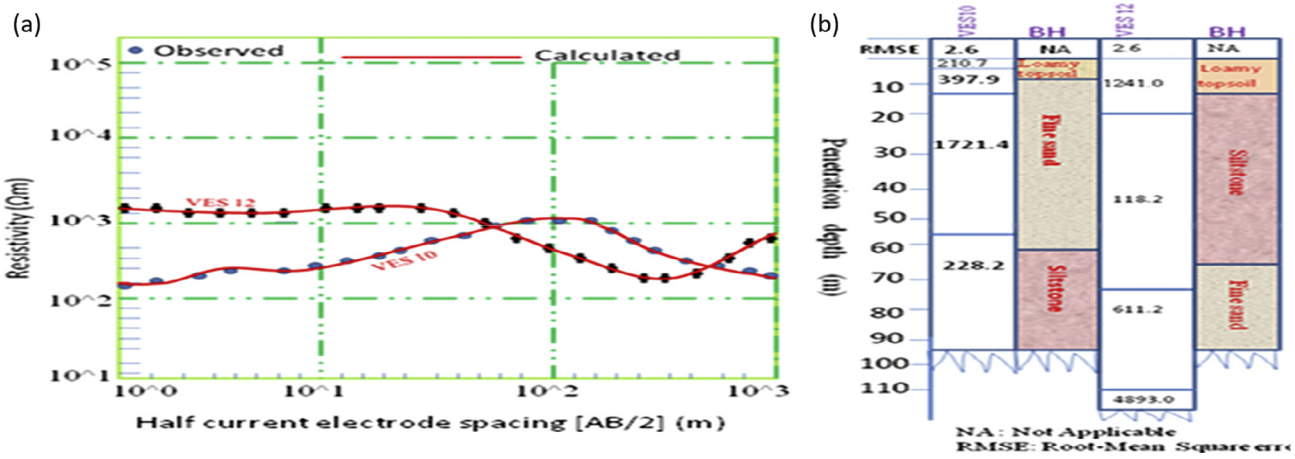

Fig. 4. Samples of modelled VES curves along CC profile (a) correlating between VES derived 1-D subsurface models and borehole lithologs (b).

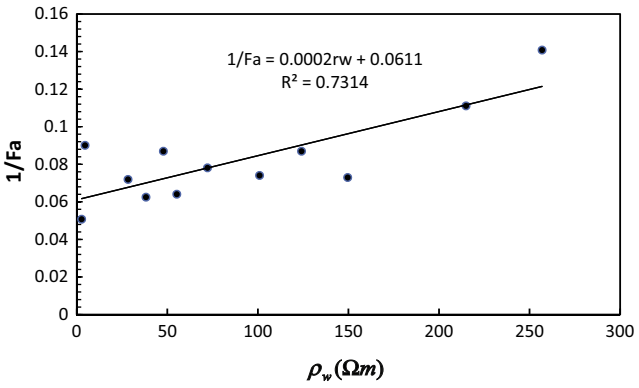

Fig. 5. A graph of inverse resistivity formation factor $\left(\frac{1}{F_a}\right)$ against pore water resistivity $(\rho_w(\Omega m))$.

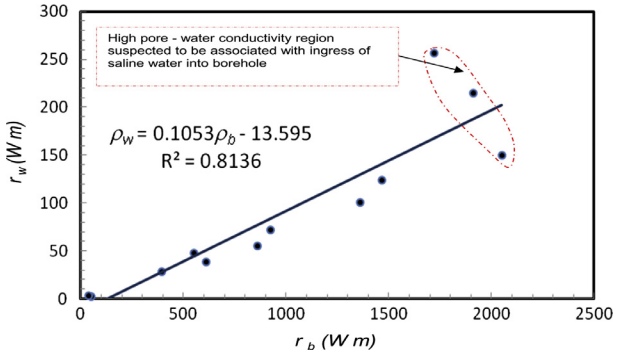

Fig. 6. A graph of aquifer pore water resistivity against formation bulk resistivity in EOLGA.

5. Data analysis, results and discussion

The field data consisting of the apparent resistivity (ρ_a) and the current electrode spacing $\left(\frac{AB}{2}\right)$ were partially curve matched, smoothened and manually plotted against each other on a bi-logarithmic scale with ρ_a on the ordinate and current electrode $\frac{AB}{2}$ on the abscissa. It was performed by either averaging the two readings at the cross over points, or deleting any outlier at the cross over points that did not conform to the dominant trend of the curve. The data point that stood out as outliers in the prevalent curve trend which could have caused serious increase in root mean square error (RMSE) during the modelling phase of the work were deleted. Where observed, such outliers constitute less than 2% of the total data generated in each sounding station and since we measured over ten data per decade, deleting such noisy data did not alter the trend of the sounding curve. Some of the deleted data might have been the electrical signatures of the thin clay materials that might have suffered suppression from the over-and underlying thick sandy aquifers (Gurunadha Rao et al., 2011; Sabet, 1975; George et al., 2011b). Any discontinuity observed in the smoothened curves was exclusively attributed to vertical variation of electrical resistivity with depth. Preliminary interpretation of the smoothened curves was made using the traditional partial curve marching technique to estimate primary layer parameters. The partial curve matching technique uses master curves and charts developed by Orellana and Mooney (1966).

A computer based VES modelling software called RESIST (Vender Velpen, 1988) that can perform automated approximation of the initial resistivity model from the observed data was later used to improve upon the preliminary interpreted results using the inversion technique. The RESIST software uses the initial layer parameters to perform some calculations and at the end generates a theoretical curve in the process. It then compares the theoretical curve with the field data curve. Since quantitative interpretation of geoelectrical sounding data is usually difficult due to the inherent problem of equivalence) (Van Overmeeren, 1989), borehole data were used to constrain all depth and minimise the choice of equiv-

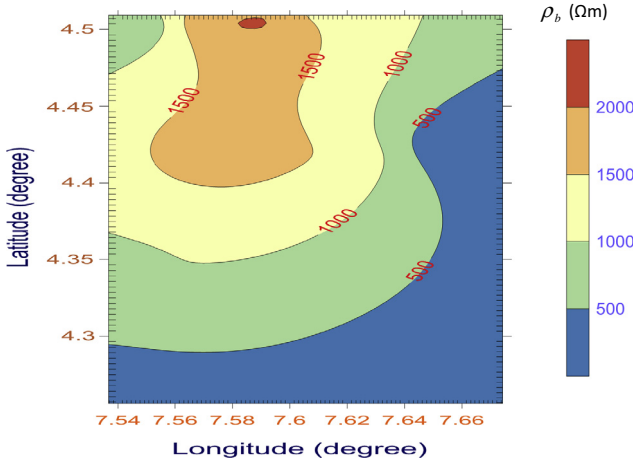

Fig. 7. Map showing the spatial distribution of bulk resistivity in EOLGA.

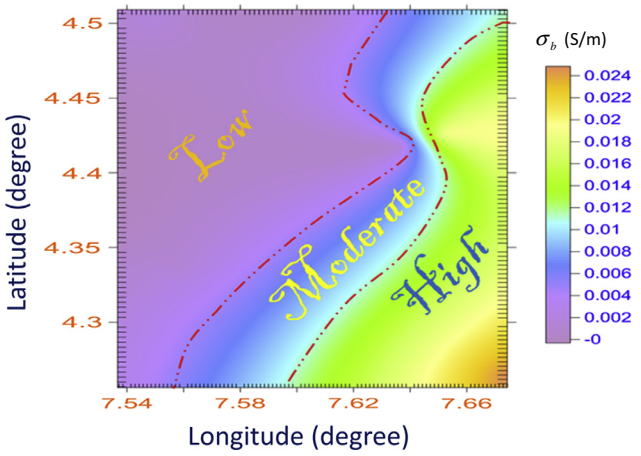

Fig. 8. Map showing the spatial distribution of bulk conductivity in EOLGA.

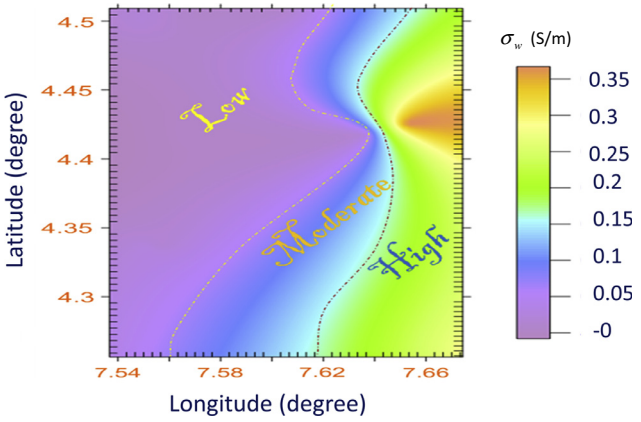

Fig. 9. Map showing the spatial distribution of water conductivity in EOLGA.

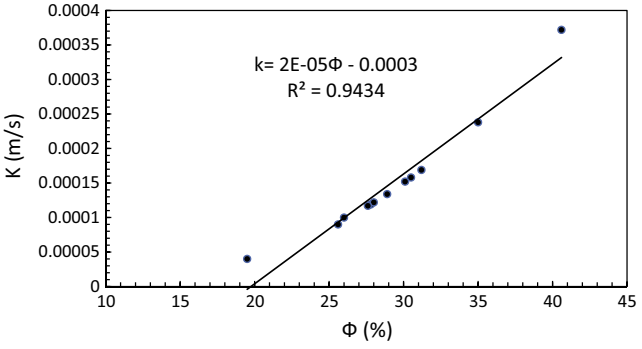

Fig. 10. A graph of hydraulic conductivity against formation bulk porosity in EOLGA.

alent models by fixing layer thicknesses and depths while allowing the resistivities to vary (Batayneh, 2009). The total number of observed minima and maxima on the smoothened VES curves were usually used as the starting number of layers (or models) over a half space for the data inversion exercise. The correlations between some of the modelled VES curves and their nearby borehole lithology interpreted results can be demonstrated in Figs. 2–4. Good correlations were observed between the borehole lithology log data and the inverted results over half space in many locations. Some minor distortions noticed in some layers were suspected to have possibly originated from the failure of the 1-D assumption of the shallow subsurface of the half space (Gurunadha Rao et al., 2011; Sabet, 1975; Obiora et al., 2015; George et al., 2016a). The result of the computer iterations gave the true layers of the subsurface penetrated by current, true resistivity of each layer, the thickness (h), depth (d) of each layer of overburden geomaterial Figs. 2–4. Three to four layers with different curve types were delineated. The availability of H and K curve types indicates the high and low values of resistivities in sediments which translate from unsaturated zones into saturated zones.

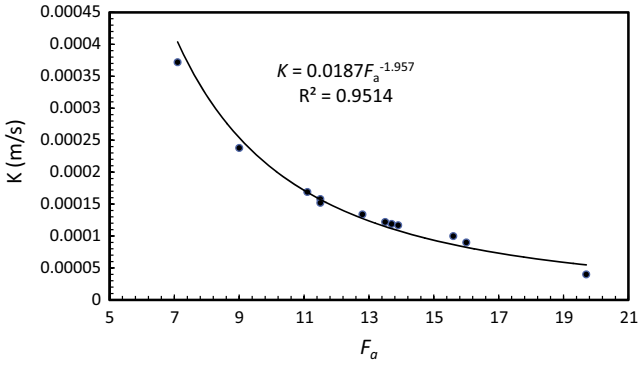

Fig. 11. A graph of hydraulic conductivity against bulk formation factor in EOLGA.

The aquifer bulk and pore - water resistivity ranged between 40.1–2049.4 Ω m (average = 995.18 Ω m) and 2.7–256.9 Ω m (average = 91.2 Ω m) respectively. These ranges respectively correspond to porosity and formation factor of (19.5–40.6%; average = 29.2%) and (7.1–19.7%; average = 12.95%). Within the standard error (δ) of 128.7 Ω m for ρ_w, 12.53 Ω m for ρ_w, 0.42 for F_a and 0.38% for ϕ, the ranges of the measured and inferred parameters according to literature reports reflect that the aquifers are sandy in nature at the indicated depths in Table 1. From KCBM equation (Eq. (11)), the hydraulic conductivity (k) was estimated with the range of 0.40×10^{-4} (3.46)–3.72×10^{-4} m/s (32.14 m/day) and average value of 1.51×10^{-4} m/s (13.04 m/day) for standard error of 0.161×10^{-4} m/s (1.8 m/day). The mean value of k coheres fairly well with the theoretically computed k value of 1.00×10^{-4} m/s reported by Niwas and de Lima (2003) for similar geologic environment.

In order to achieve the purpose of this study, geostatistical analysis of field data and data analysed in the laboratory from aquifer sediments were performed. The data were also contoured in order to assess their spatial distribution, which enabled us to assess the lateral spread of the measured/inferred data in the study area. The aquifer surface conductivity of residual clay was also estimated through the plot of $\frac{1}{F_a}$ against ρ_w in Eq. (6) (see Fig. 5). The intercept of the graph signifies the intrinsic aquifer formation factor F_i, (clay-free formation factor) whose estimated value from the graph is 16.339. The numerical value of the surface conductivity BQ_v was estimated to be 3.2679×10^{-3} Siemens/metre (3.2679 mS/m) through the slope - intercept relationship. The magnitude of surface conductivity (σ_A) of argillaceous bands usually neglected can have a multiplier effect on the aquifer bulk conductivity (σ_b), and is therefore serving as a correction factor to any petrophysical measurements that uphold Archie's model in the study area. Based on this study, Sen et al. (1998) in Eq. (12), shows that σ_b of aquifer repositories, is a composition of conductivity of clean sands and conductivity of residual clay is suggested for the area.

$$\sigma_b = \frac{\sigma_w \cdot \phi^m}{a} + \sigma_A \tag{12}$$

Substituting the estimated σ_A, Eq. (13) leads to Eq. (12):

$$\sigma_b = \frac{\sigma_w \cdot \phi^m}{a} + 3.2679 \text{ mS/m} \tag{13}$$

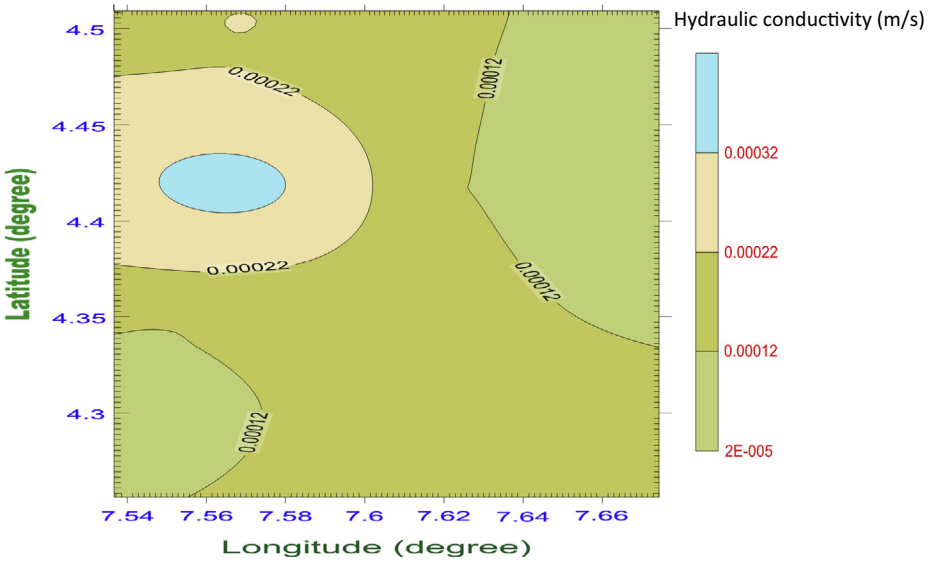

Fig. 12. Map showing the spatial variation of hydraulic conductivity in EOLGA.

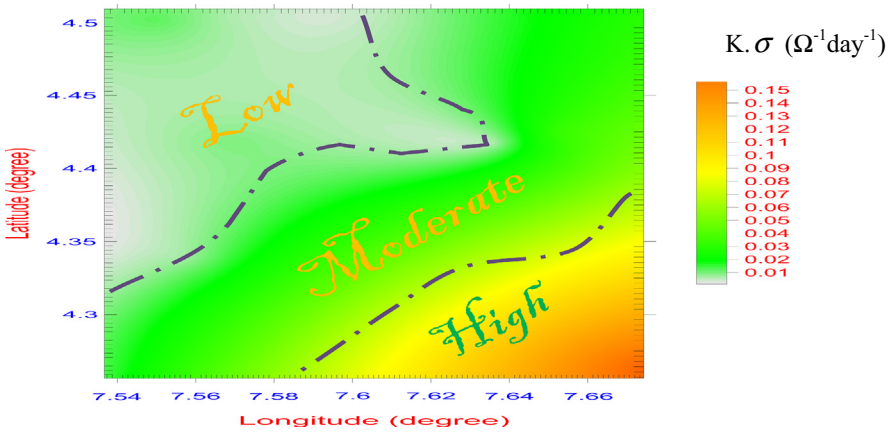

Fig. 13. Map showing the spatial distribution of $k \cdot \sigma$ in EOLGA.

The fine-coarse sands and the siltstones aquifers that dominate the study area have argillaceous bands that put additional charge carriers in the fluid adjacent to the solid surfaces, causing additional, additive term of electrical conductivity of 3.2679 mS/m. For clay-free sands assumed by Archie's model, this value of conductivity must be subtracted from σ_b in order to ensure the workability of Archie's assumption. On the basis of Eq. (13) we would anticipate $\sigma_{clay} > \sigma_{silt} > \sigma_{sand}$ when clay dominates over the aquifer system since clay conducts more than silt and sand. However, since the argillaceous bands contain small amount of irreducible clay in clean sands considered here, the bulk sand resistivity is higher.

In a typical petrophysical aquifer sediment formation assessment, interpretation of conductivity would not be undertaken in the absence of additional control or *apriori* information. Therefore, the site dependent corrective term of conductivity σ_A, estimated as 3.2679 mS/m is valuable. The application of this procedure has provided new information on the conductivity characteristics of aquifer systems in EOLGA. It would appear that the response of the residual clay-shale group sediments in economic aquifer sands is particularly sensitive to rapid changes in the second term of Eq. (12). It can be argued that the observed spatial responses are due to clay content since the shale is known to be organic-rich (Huntley, 1987).

The scatterings/outliers observed in the plot between $\frac{1}{F_a}$ and ρ_w are due to the variations in grain size of sediments, anisotropy and facies change. From the regression with correlation coefficient, $R^2 = 0.7314$ given in Eq. (14) below, the intrinsic (clean sand) fractional porosity, was estimated to be 0.204 (20.4%) using the intercept (intrinsic formation factor F_i) of Eq. (6).

$$\frac{1}{F_a} = 0.0002\rho_w + 0.0612 \tag{14}$$

The plot of formation water resistivity against bulk water resistivity with good correlation ($R^2 = 0.8136$) in Fig. 6 shows direct proportionality with the characteristic equation given in Eq. (15).

$$\rho_w = 0.1053\rho_a - 13.595 \tag{15}$$

However, the observed outliers, mostly in the ringed segment of the regression line are suspected to be due to variation in the residual intercalated argillaceous bands present in the aquifer formations and ingress of saline water into the borehole at the location indicated by the coordinates on Table 1. This graph shows that the bulk resistivity, the converse of bulk conductivity of both sand and argillaceous bands increases proportionally with the formation water resistivity. The spatial variations in magnitude of bulk resistivity/conductivity and that of water resistivity are shown if

Figs. 7–9 respectively. The maps in Figs. 8 and 9 show conformity in agreement with Figs. 6 and 7 shows increase in the reverse order of magnitude when compared with Figs. 8 and 9. The spatial displays in Figs. 7 and 8 depict three zones corresponding to low, moderate and high values of conductivities. These zones show interplay between sands and argillaceous bands within the aquifer repositories in EOLGA. The magnitude of latent clay contents which were not revealed in VES are more concentrated in a decreasing order from high, moderate and low zones displayed on the maps. Therefore, the major contributors of σ_A are the zones on the maps with high conductivities. The hydraulic conductivity estimated using Eq. (11) was also plotted against porosity of the aquifers. The display in Fig. 10 shows a linear and increasing relationship characterized by the equation given in Eq. (16) with good correlation coefficient (R^2 = 0.9434).

$$k = 1.5911\phi - 31.421 \tag{16}$$

The relation between k and ϕ shows that as k increases ϕ also increases in the aquifer. This equation can be used to predict k in the study area and similar geology within the neighbourhood. In the same vein, aquifer hydraulic conductivity was plotted against bulk formation factor as shown in Fig. 11. From the regression analysis, a power law with characteristic equation that k decreases with F_a exponentially resulted as shown in Eq. (17) with high correlation coefficient (R^2 = 0.9514);

$$k = 0.0187F_a^{-1.957} \tag{17}$$

The above relation gives the behaviour of k and F_a in the aquifer and can be used to obtain more values of k at any location of EOLGA when F_a is known for the same geology. The estimated values of k were contoured as shown in Fig. 12. The distribution of k at different VES locations shown on the map can serve as a guide in groundwater flow modeling in EOLGA. Generally, k increases towards the western section of the map on the average as the contour lines show. Although there are other factors that affect k, the distribution of k on the map is depends on the porosity as high porosity means high k.

The spatial distribution of $k \cdot \sigma$ values (see Table 1) and Fig. 13 is in support of the nearly homogeneous spread of the sandy aquifers across the entire area with no significant change in the composition of the pore fluid content. However, the changes classified into low, moderate and high values of $k \cdot \sigma$ are due to the argillaceous bands in the sandy aquifers considered which have higher concentrations at the south-eastern section of the map in Fig. 13. The observed disparity in $k \cdot \sigma$ values displayed on the map can equally be used in contamination studies.

6. Conclusion

In a typical sediment assessment, interpretation of conductivity should be focused on sands and the argillaceous bands imbedded on the sediments no matter how clean the sands may be. Given the extensive nature of electrical surveys and their inherent mapping functionality, it seems natural to classify, and hence simplify, the spatially aggregated conductivity information on the basis of sediment lithology. Such attribution provides an inherent link between lithological sediment parameters and the petrophysical parameters controlling bulk conductivity. The procedure also adds a significant degree of control in relation to the interpretation of the conductivity variations. Accepting that the bulk conductivity is contributed by sands and argillaceous bands and correcting it by subtracting the conductivity caused by argillaceous bands from bulk conductivity will reduce the aberrations in interpretations usually encountered when Archie's law is assumed. Besides, acknowledging the increasing conductivity due to unseen pore-scale clays in aquifer sediments and correcting this anomaly could be useful in deriving near error free input parameters for contaminant migration modelling and in improving the quality of model. Given the observations discussed here, the interplay between the sand conductivity and argillaceous band conductivity which give rise to bulk conductivity of aquifer systems can be a model for the study of electrical conductivity and transport properties of pore systems at nanometre scale. Groundwater flow study in the area is necessary in order to check for the level of saltwater- freshwater interactions mostly within the ambient of VES points characterised with high disparity in $\rho_w - \rho_b$ plot ringed in Fig. 6.

Acknowledgments

We are grateful to Millennium Development Goal Initiative for sponsoring and providing the first author with the water and cored geological samples that were used in the study. We are indeed grateful to University of Calabar, Cross River State, Nigeria for providing the Terrameter and its accessories used in acquiring the VES data. We are also thankful to Dr. Anthony E. Akpan who made the RES1D software that was used in modelling some of the VES data freely available for research purposes. The first author is equally indebted to his wife, Mrs. Precious N. George for granting a safe environment for the manuscript to be written. Thanks are also due to all the anonymous reviewers for their comments, suggestions and thorough reviews which have greatly improved the quality of the original manuscript.

References

Akwa Ibom State Millennium Development Goal (AKSMDG), 2011. Borehole Completion report from the thirty one Local Government Areas of Akwa Ibom State, Nigeria. Technical Report, 355pp.

Alger, R.P., 1966. Interpretation of Electric Logs in Fresh Water Wells in Unconsolidated Formations. Society of Prof Well Log Analyst Trans, Art CC, pp. 1–25.

American Petroleum Institute, API, 1960. Recommended practice for core analysis procedure. Report No. 40, pp. 55.

Archie, G.E., 1942. The Electrical Resistivity Log as an Aid in Determining Some Reservoir Characteristics. American Institute of Mineral and Metal Engineering. Technical publication 1422, Petroleum Technology, pp. 8–13.

Aristodemou, E., Thomas-Betts, A., 2000. DC resistivity and induced polarisation investigations at a waste disposal site and its environments. J. Appl. Geophys. 44, 275–302. PII: S0926-9851_99.00022-1.

Batayneh, A.T., 2009. A hydrogeophysical model of the relationship between geoelectric and hydraulic parameters, central Jordan. J. Water Resour. Prot. 1, 400–407. http://dx.doi.org/10.4236/jwarp.2009.16048.

Benkabbour, B., Toto, E.A., Fakir, Y., 2004. Using DC resistivity method to characterize the geometry and the salinity of the Plioquaternary consolidated coastal aquifer of the Mamora plain, Morocco. Environ. Geol. 45, 518–526. http://dx.doi.org/10.1007/s00254-003-0906-y.

Carothers, J.E., 1968. A statistical study of the formation factor relation. Log Anal. 9 (5), 13–20.

Chambers, J.E., Wilkinson, P.B., Wealthall, G.P., Loke, M.H., Dearden, R., Wilson, R., Allen, D., Ogilvy, R.D., 2010. Hydrogeophysical imaging of deposit heterogeneity and groundwater chemistry changes during DNAPL source zone bioremediation. Journal of Contaminant Hydrology 118, 43–61.

Edet, A.E., Worden, R.H., 2009. Monitoring of the physical parameters and evaluation of the chemical composition of river and groundwater in Calabar (Southeastern Nigeria). Environ. Monit. Assessment 157, 243–258. http://dx.doi.org/10.1016/j.jconhyd.2010.07.001.

Emerson, D.W., 1969. Laboratory electrical resistivity measurements of rocks. Proc. Aust. Inst. Mining Metall. 230, 51–62.

Farauta, B.K., Egbule, C.L., Agwu, A.E., Idrisa, Y.L., Onyekuru, N.A., 2012. Farmers' adaptation initiatives to the impact of climate change on agriculture in Northern Nigeria. J. Agric. Extension 16, 132–144. http://dx.doi.org/10.4314/jae.v16i1.13.

Fetters, C.W., 1994. Applied Hydrogeology. Prentice Hall Inc, New Jersey.

Frohlich, R.K., Urish, D.W., 2002. The use of geoelectrics and test wells for the assessment of groundwater quality of a coastal industrial site. J. Appl. Geophys. 50, 261–278. PII: S0926-985102)00146-5.

Galehouse, J.S., 1971. Sedimentation analysis. In: Carver, R.F. (Ed.), Procedures in Sedimentary Petrology. Wiley-Interscience, New York, p. 653.

George, N.J., Akpan, A.E., Obot, I.B., 2010. Resistivity study of shallow aquifer in parts of southern Ukanafun Local government area, Akwa Ibom State. E- J. Chem. 7 (3), 693–700.
George, N.J., Obianwu, V.I., Obot, I.B., 2011a. Estimation of groundwater reserve in unconfined frequently exploited depth of aquifer using a combined surficial geophysical and laboratory techniques in the Niger Delta, Southern Nigeria. Adv. Appl. Sci. Res. 2 (1), 163–177.
George, N.J., Obinawu, V.I., Udofia, K.M., 2011b. Estimation of aquifer hydraulic parameters via complementing surficial geophysical measurement by laboratory measurements on the core samples in southern part of Akwa Ibom State, Nigeria. Int. Rev. Phys. 5 (2), 88–97.
George, N.J., Ekong, U.N., Etuk, S.E., 2014a. Assessment of economically accessible groundwater reserve and its protective capacity in Eastern Obolo Local Government Area of Akwa Ibom State, Nigeria, using electrical resistivity method. Int. J. Geophys., 1–10 http://dx.doi.org/10.1155/2014/578981.
George, N.J., Ubom, A.I., Ibanga, J.I., 2014b. Integrated approach to investigate the effect of leachate on groundwater around the Ikot Ekpene Dumpsite in Akwa Ibom State, South-eastern Nigeria. Int. J. Geophys., 1–10 http://dx.doi.org/10.1155/2014/174589.
George, N.J., Ibanga, J.I., Ubom, A.I., 2015. Geoelectrohydrogeological indices of evidence of ingress of saline water into freshwater in parts of coastal aquifers of Ikot Abasi, southern Nigeria. J. African Earth Sci. 109, 37–46. http://dx.doi.org/10.1016/j.jafrearsci.2015.05.001.
George, Nyakno J., Akpan, Anthony E., Evans, Udoh F., 2016a. Prediction of geohydraulic pore pressure gradient differentials for hydrodynamic assessment of hydrogeological units using geophysical and laboratory techniques: a case study of the coastal sector of Akwa Ibom State, Southern Nigeria. Arabian J. Geosci. 9 (4), 1–13.
George, N.J.A., Akpan, A.E., Ekanem, A.M., 2016b. Assessment of textural variational pattern and electrical conduction of economic and accessible quaternary hydrolithofacies via geoelectric and laboratory methods in SE Nigeria: a case study of select locations in Akwa Ibom State. J. Geol. Soc. India 88 (4), 517–528.
Gomaa, M.M., 2013. Forward and inverse modeling of the electrical properties of magnetite intruded by magma, Egypt. Geophys. J. Int. 194 (3), 1527–1540.
Gomaa, M.M., Abou, El-Anwar E., 2015. Electrical and geochemical properties of tufa deposits as related to mineral composition in South Western Desert, Egypt. J. Geophys. Eng. 12 (3), 292–302.
Gowd, S.S., 2004. Electrical resistivity surveys to delineate groundwater potential aquifers in Peddavanka watershed, Anantapur District, Andhra Pradesh, India. Environ. Geol. 46, 118–131. http://dx.doi.org/10.1007/s00254-004-1023-2.
Gurunadha Rao, V.V.S., Tamma Rao, G., Surinaidu, L., Rajesh, R., Mahesh, J., 2011. Geophysical and geochemical approach for seawater intrusion assessment in the Godavari Delta Basin, A.P., India. Water, Air Soil Pollut. 217, 503–514. http://dx.doi.org/10.1007/s11270-010-0604-9.
Hill, H.J., Milburn, J.D., 1956. Effects of clay and water salinity on electrochemical behaviour of reservoir rocks. Trans. AIME 207, 65–72.
Huntley, D., 1987. Relations between permeability and electrical resistivity in granular aquifers. Ground Water 24 (4), 466–474. http://dx.doi.org/10.1111/j.1745-6584.1986.tb01025.x.
Ibanga, J.I., George, N.J., 2016. Estimating geohydraulic parameters, protective strength, and corrosivity of hydrogeological units: a case study of ALSCON, Ikot Abasi southern Nigeria. Arabian J. Geosci. 9 (5), 1–16.
Keller, G.V., Frischknecht, F.C., 1966. Electrical Methods in Geophysical Prospecting. Pergamon, London, p. 517.
Khalil, M.A., Abd-Alla, M.A., 2005. An approach to estimate hydraulic parameters and water quality from surface resistivity measurements at wadi El-Assuity area, Egypt. NRIAG J. Geophys., Special Issue, 267–281.
Kirsch, R., 2009. Groundwater quality-saltwater intrusions. In: Kirsch, R. (Ed.), Groundwater Geophysics: A Tool for Hydrogeology. Springer-Verlag, Berlin Heidelberg. http://dx.doi.org/10.1007/978-3-540-88405-7. second ed..
Martínez, A.G., Takahashi, K., Núñez, E., Silva, Y., Trasmonte, G., Mosquera, K., Lagos, P., 2008. A multi-institutional and interdisciplinary approach to the assessment of vulnerability and adaptation to climate change in the Peruvian Central Andes: problems and prospects. Adv. Geosci. J. 14, 257–260.
Nganje, T.N., Edet, A.E., Ekwere, S.J., 2007. Concentrations of heavy metals and hydrocarbons in groundwater near petrol stations and mechanic workshops in Calabar metropolis, southeastern Nigeria. J. Environ. Geosci. 14 (1), 15–29. http://dx.doi.org/10.1306/eg.08230505005.
Niwas, S., de Lima, O.A.L., 2003. Aquifer parameter estimation from surface resistivity data. Groundwater 41 (1), 94–99.
Obiora, D.N., Ibuot, J.C., George, N.J., 2015. Evaluation of aquifer potential, geoelectric and hydraulic parameters in Ezza North, southeastern Nigeria, using geoelectric sounding. Int. J. Environ. Sci. Technol. http://dx.doi.org/10.1007/s13762-015-0886-y.
Orellana, E., Mooney, A.M., 1966. Master Curve and Tables for Vertical Electrical Sounding Over Layered Structures. Interciencia, Escuela, Spain.
Ransom, R.C., 1984. A contribution towards a better understanding of the modified Archie formation resistivity factor relationship. The Log Analyst, 7–12.
Rapti-Caputo, D., 2010. Influence of climatic changes and human activities on the salinization process of coastal aquifer systems. Italian J. Agronomy/River Agronomy 3, 67–79.
Reijers, T.J.A., Petters, S.W., 1987. Depositional environment and diagenesis of Albian carbonates in Calabar Flank, S. E. Nigeria. J. Pet. Geol. 10, 283–294.
Riddell, E.S., Lorentz, S.A., Kotze, D.C., 2010. A geophysical analysis of hydro-geomorphic controls within a headwater wetland in a granitic landscape, through ERI and IP. J. Hydrol. Earth Syst. Sci. 14, 1697–1713. http://dx.doi.org/10.5194/hess-14-1697-2010.
Rivett, M.O., Clark, L., 2007. A quest to locate sites described in the world's first publication on trichloroethene contamination of groundwater. Q. J. Eng. Geol. Hydrogeol. 40, 241–249.
Roy, K.K., Elliot, H.M., 1981. Some observations regarding depth of exploration in DC electrical methods. Geoexploration 19, 1–13.
Sabet, M.A., 1975. Vertical electrical resistivity sounding locate groundwater resources: a feasibility study. Virginia Polytechnical Institute. Water Resour. Bull. 73, 63.
Schön, J.H., 1996. Physical Properties of Rocks: Fundamentals and Principles of Petrophysics. Pergamon Press, New York.
Sen, P.N., Goode, P.A., Sibbit, A., 1998. Electrical conduction in clay bearing sandstones at low and high salinities. J. Appl. Phys. 63, 4832–4840.
Singh, K.P., 2005. Nonlinear estimation of aquifer parameters from surficial resistivity measurements. J. Hydrol. Earth Syst. Sci. Discuss. 2, 917–938. SRef-ID: 1812-2116/hessd/2005-2-917.
Slater, L., 2007. Near surface electrical characterization of hydraulic conductivity: from petrophysical properties to aquifer geometries—a review. Surveys Geophys. 28, 169–197. http://dx.doi.org/10.1007/s10712-007-9022-y.
Soupios, P.M., Kouli, M., Vallianatos, F., Vafidis, A., Stavroulakis, G., 2007. Estimation of aquifer hydraulic parameters from surficial geophysical methods: a case study of Keritis Basin in Chania (Crete – Greece). J. Hydrol. 338, 122–131. http://dx.doi.org/10.1016/j.jhydrol.2007.02.028.
Tait, N.G., Lerner, D.N., Smith, J.W.N., Leharne, S.A., 2004. Prioritisation of abstraction boreholes at risk from chlorinated solvent contamination on the UK Permo-Triassic Sandstone aquifer using a GIS. Sci. Total Environ. 319 (1–3), 77–98.
Van Overmeeren, R., 1989. Aquifer boundaries explored by geoelectrical measurements in the coastal plain of Yemen: a case study of equivalence. Geophysics 54, 38–48.
Vender Velpen, B.P.A., 1988. A computer processing package for D.C. Resistivity interpretation for an IBM compatibles. ITC Journal 4, The Netherlands.
Vinegar, H.J., Waxman, M.H., 1984. Induced polarization of Shaly Sands. Geophysics 49 (8), 1267–1287. http://dx.doi.org/10.1190/1.1441755.
Wagner, G., Zeckhauser, R.J., 2011. Climate policy: hard problem, soft thinking. Climatic Change. http://dx.doi.org/10.1007/s10584-011-0067-z.
Waxman, S.H., Smits, L.J.M., 1968. Electrical conductivities in oil-bearing sands. J. Soc. Pet. Eng. 8, 107–122.
Worthington, P.F., 1993. The uses and abuses of the Archie's equation: the formation factor – porosity relationship. J. Appl. Geophys. 30, 215–228.
Zhdanov, M.S., Keller, G., 1994. The Geoelectrical Methods in Geophysical Exploration, Methods in Geochemistry and Geophysics. Elsevier.